PHYSICAL REVIEW B VOLUME 39, NUMBER 16 1 JUNE 1989

Grain-boundary ordering, segregation, and melting transitions in a two-dimensional lattice-gas model

D. Farkas and H. Jang
Department of Materials Engineering, Virginia Polytechnic Institute and State University, Blacksburg, Virginia 24061
(Received 5 May 1988; revised manuscript received 3 January 1989)

A two-dimensional lattice-gas model of a binary-ordering-alloy system was used to study the phase transitions and the atomic configuration near a $\Sigma=5$ grain boundary. The cluster variation method was used to study order-disorder and melting transitions in the bulk alloys. The complete binary phase diagrams were constructed for two different sets of interaction-energy assumptions. Simulations based on the same model were performed to study these transitions in the grain-boundary region. In addition, the model also yields information on the segregation behavior of the alloying elements in the grain-boundary region.

I. INTRODUCTION

In recent years there has been significant interest in the development of ordered alloys as new materials for high-temperature use. Particular interest has been devoted to the grain-boundary region, since most of these materials fail intergranularly. Furthermore, it has been shown that minor changes in the chemistry of the grain-boundary region can dramatically change its mechanical properties. It is therefore very important to theoretically understand the particular features of the grain-boundary structure in ordered alloys. However, most of the theoretical studies of grain-boundary structure are performed using energy-minimization techniques at absolute zero. In the few high-temperature studies of pure materials there has been some evidence of the possibility of melting transitions of grain boundary at temperatures below the bulk melting point.[1,2,3] Other calculations show significant disordering and segregation effects near a free surface or an antiphase boundary.[4,5] Monte Carlo calculations have been carried out for grain boundaries[5] showing significant variation of the antisite defect near the grain-boundary region. It may be expected that at high temperatures these effects will be significant in controlling the grain-boundary behavior. The purpose of the present work is to study the possible disordering and segregation effects near a $\Sigma=5$ grain boundary at high temperatures. In particular, we are interested in studying the influence of important features of the bulk behavior on the grain-boundary structure, for example, the effects of a large difference in the melting points of the two components of the binary alloy.

The model used is similar to that of Kikuchi and Cahn for a pure material[1] and is extended by us for two components. The model is very simple and two dimensional. It can, nevertheless, yield general trends which are expected to be valid in a wide variety of cases. Although two-dimensional results will not be necessary over to the three-dimensional case, the simple model is particularly useful in studying the relationship of the obtained results to the energetic assumptions in the model.

Both disordering and segregation behavior will be strongly related to the energetic assumptions in the model. In Sec. II A we discuss the assumptions chosen in the present work. The cases studied are restricted to those for which the low-temperature structure of the boundary is perfectly solid and well ordered. These features, as well as the low-temperature segregation behavior are discussed in Sec. II B. As the temperature increases, the boundary increasingly becomes both chemically and spatially disordered. All cases studied are for an ordering alloy with a bulk order-disorder temperature lower than the melting point, which means that the dominant type of transition in the grain boundary will be chemical disordering and segregation. One particular feature of the structure of grain boundaries in ordered alloys is the fact that different ordering configurations are possible. These do not have necessarily the same energy. The present model alloys the study of the different ordering configurations in the grain-boundary region and their energy. We have restricted the present study to configurations that are actually coincident-site structures. In the nomenclature of Takasugi and Izumi[6] these are called fully symmetrical boundaries, as opposed to what they call pseudosymmetrical boundaries. Also, no rigid-body translations of one crystal with respect to the other were allowed. Transitions among the different structures are observed in the calculations. These different types of transitions are discussed in Sec. II C.

The study of the full phase diagrams corresponding to each of the energy assumptions is essential to fully understand the grain-boundary region and is undertaken first. These results are reported in Sec. III A. Section III B includes the results for the grain-boundary ordering transitions, and Sec. III C describes the observed segregation behavior.

II. THEORY

A. The model and interaction-energy assumptions

The present model is based on a two-dimensional lattice gas with the same assumptions as in Ref. 1. The energy computation is performed on a pairwise basis, and

only two possible interatomic distances are included. One of these distances corresponds to the bulk nearest-neighbor distance and the other is slightly larger. The two distances are indicated in Fig. 1 as AB and AC, respectively. The ratio of the interaction energies corresponding to the two distances is a measure of the shape of the interatomic potential and may influence the results. In the present work we have used the same ratio as in Ref. 1, namely 1.2, meaning that the interaction energy for the larger distance is 20% smaller than the interaction at nearest-neighbor distances. In the present work this assumption is maintained for both components and the cross interaction energies as well. Kikuchi and Cahn[7] recently reported a study of the influence of varying this assumption differently for the different types of interactions. In the present work, we studied the effect of an asymmetry in the phase diagram and therefore maintained other parameters constant. Interactions at distances lower than the nearest-neighbor distance are not allowed, that is, they are strongly repulsive. Interactions at distances larger than AC in Fig. 1 are taken as zero and not included in the calculations.

In addition, we assume an ordering system with an ordering energy,

$$V=\varepsilon_{AB}-\frac{\varepsilon_{AA}+\varepsilon_{BB}}{2} .$$

Two different cases were tested in the calculations corresponding to two different phase diagrams. The first one is that of a completely symmetric phase diagram where the melting points of the two components are the same. The second one is that of an asymmetric diagram where one of the components has a higher melting point than the other. These cases correspond to two different values of the energy parameter, defined as

$$\Delta=\frac{\varepsilon_{AA}-\varepsilon_{BB}}{V} .$$

The value $\Delta=0$ corresponds to a symmetric phase diagram and the value $\Delta=1.33$ corresponds to a phase diagram that is asymmetric with a lower melting point of component B. The ordering energy is maintained the same for both cases. Table I summarizes the assumptions used for the energy calculation.

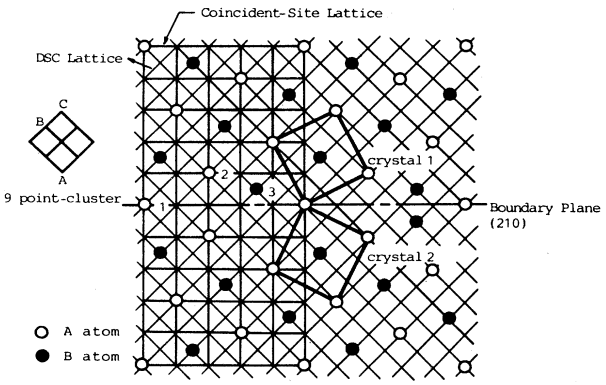

FIG. 1. The structure of a two-dimensional $\Sigma=5$ grain boundary and the nine-point basic cluster in the model.

TABLE I. Summary of the assumptions used for the energy calculation.

	Δ	V/ε_0	μ_A/ε_0	μ_B/ε_0
Case 1[a]	0.00	0.45	−1.5	−1.5
Case 2[b]	1.33	0.45	−2.22	−0.78

[a]Stoichiometric alloy in a symmetric phase diagram.
[b]Stoichiometric alloy in an asymmetric phase diagram.

For the calculation of the entropy the cluster variation method was used with a basic cluster of nine points. Since distances lower than the nearest neighbor are not allowed, at most two out of the nine points in the cluster can be occupied. This reduces the number of possible configurations of the cluster that have to be considered in the calculation of the entropy. The total number is 59 configurations of the basic cluster. The geometry of this cluster allows the calculation of the free energies for bulk solid and liquid phases as well as for $\Sigma=5$ grain boundary. The minimization of the free energy is then carried out for each of these cases with respect to the equilibrium distribution of each of the possible configurations of the basic cluster.

The different bulk phases and the grain boundary have different symmetry constraints that have to be considered in the calculation. For all the bulk phases neither cluster distributions nor chemical concentrations are fixed. Rather the chemical potential of both species is fixed, and the minimization process yields the equilibrium configurational distribution and concentration. A number of lattice planes have to be considered for all phases. For the solid phases, five points per plane are considered, as shown in Fig. 1. The number of lattice planes is at least 10 for the bulk solid phases. We used 15 for all bulk phases. As the minimization proceeds, the configurations in planes n and $n+10$ are maintained equal. For the grain boundary the number of planes needs to be much larger since the periodicity is broken in the direction perpendicular to the boundary. We used at least 37 planes in this case. The configuration of the planes far from the boundary is fixed and set equal to the bulk equilibrium configuration at that temperature and for the same chemical potentials. The numerical method used for the minimization is natural iteration, as described by Kikuchi.[8]

B. Low-temperature behavior

The low-temperature behavior of the system is readily understood based on the energetic assumptions described above. The stable bulk phase at low temperature will be the ordered solid, and there are two equivalent variants of this ordered solid which are the ones shown as upper and lower crystals in Fig. 1.

The low-temperature structure of the boundary will be determined by the fact that distances closer than nearest

neighbor are not allowed. This means that one atom per boundary period has to disappear. This will occur in the two planes that are immediately adjacent to the grain-boundary plane in both crystals giving rise to the W-shaped density of the boundary found by Kikuchi in the pure material. In the case of the ordered alloy with the energetic assumptions discussed above the grain-boundary region will be ordered at low temperatures. There will be two possible configurations of this low-temperature ordered boundary corresponding to the location of the boundary plane at a plane of A or B atoms, respectively. For the case of a symmetric phase diagram these two configurations will be equivalent, not so in the case where the two melting points differ. In this later case the boundary located at a plane of (low-melting-point) B atoms will be lower in energy.

The segregation behavior at low temperatures is determined by the shape of the potential, i.e., the assumption that the interaction energies at distances AC of Fig. 1 is 20% lower than that of nearest neighbors, and the fact that this assumption is also maintained for the cross interactions in the ordering system. It can be shown easily that for both pure A and pure B the other type of atom present as impurities will be rejected from the boundary. This is seen if the energies associated with a B impurity in pure A are calculated for the different locations of the impurity. These are as follows: (1) the B atom located in the bulk consisting mainly of A atoms, $1.2\times4(\varepsilon_{AB}-\varepsilon_{AA})$; (2) the B atom located at sites 1 or 3 in the grain boundary, $1.2\times3(\varepsilon_{AB}-\varepsilon_{AA})$; (3) the B atom located at grain boundary site 2, $(1.2\times3+1)(\varepsilon_{AB}-\varepsilon_{AA})$; where sites 1, 2, and 3 refer to the ones indicated in Fig. 1. For the symmetric energy parameter ($\varepsilon_{AA}=\varepsilon_{BB}>\varepsilon_{AB}$) it is clear that the bulk is the energetically most favorable location, and the impurity will therefore be rejected from the boundary. A similar reasoning yields the conclusion that A impurities in pure B will also be rejected from the boundary. Since in the stoichiometric alloy of case 1 in Table I, A and B are completely equivalent in this case, there will be no segregation. On the other hand, in the stoichiometric alloy of case 2 in Table I the boundary will be enriched in the lower-melting-point element since $\varepsilon_{AA}>\varepsilon_{BB}>\varepsilon_{AB}$.

C. Types of transitions

The first type of transition that can be observed in the present model is the order-disorder transitions in the bulk and in the grain-boundary region. The order-disorder transition in the two-dimensional model used here is of second order for all compositions, since both ordered and disordered phases will have very few vacancies at temperatures close to the transition. It is expected that the calculated transition behavior for the bulk will be the same as that predicted by a two-dimensional square Ising model in the pair approximation. The critical issue is the order-disorder behavior in the grain-boundary region. It is possible that this transition will be different from that of the bulk. Previous work studying the order-disorder phenomena near the surface region observed that the surface region is more disordered than the bulk.[4] Two types of transitions have been observed.[9] The first one, called ordinary, is one where the actual order-disorder temperature of the surface is the same as in the bulk, even if the surface region is more disordered than the bulk at temperatures below the transition. The second one is called an extraordinary transition, where the temperatures are different.

In addition to the order-disorder temperatures the present model can study melting transitions. These are of first order in the bulk and have been shown to occur in the boundary region at temperatures lower than the melting point of the bulk. These types of transitions are clearly evident in the density profiles of the boundary at high temperatures, as shown by Kikuchi and Cahn[1] for a pure material. In the present model it is important to note that as we move in composition it is essential to maintain constant pressure in the calculations, and since vacancies are included in significant amounts close to the melting point, this condition is not necessarily maintained. The Gibbs-Duhem equation has to be satisfied as composition changes, as described below in the calculation of the phase diagrams.

Finally, it is interesting to study the transition that occurs among the different possible grain-boundary structures. This is the case in the asymmetric phase diagram, where the two possible locations of the grain-boundary plane are not equivalent and a transition among them may occur. For this transition to occur the boundary plane has to shift a total of five planes to the next coincident-site plane.

III. RESULTS

A. Phase-diagram calculation

The phase diagram for a pure component has already been calculated using the present model by Kikuchi and Cahn[1] and will not be reproduced here. We have calculated the binary diagrams corresponding to the two different energetic assumptions listed in Table I. The diagrams were constructed as it is usually done in cluster-variation calculations, that is calculating the grand potential for the different phases. The difficulty in constructing binary diagrams with the present model is that since vacancies are included, it is necessary to insure that the coexistence temperatures for different compositions are calculated at constant pressure. In order to do this we started with the stoichiometric compound and moved away from the equiatomic composition in small enough steps so as to satisfy the Gibbs-Duhem equation at constant pressure:

$$\sum_i X_i\mu_i=0 .$$

The size of the steps was found to be of a few percent, and decreasing the steps further did not change the results. Figures 2 and 3 show the computed complete diagrams for both cases mentioned in Table I. For the stoichiometric alloy of case 1 we used a chemical poten-

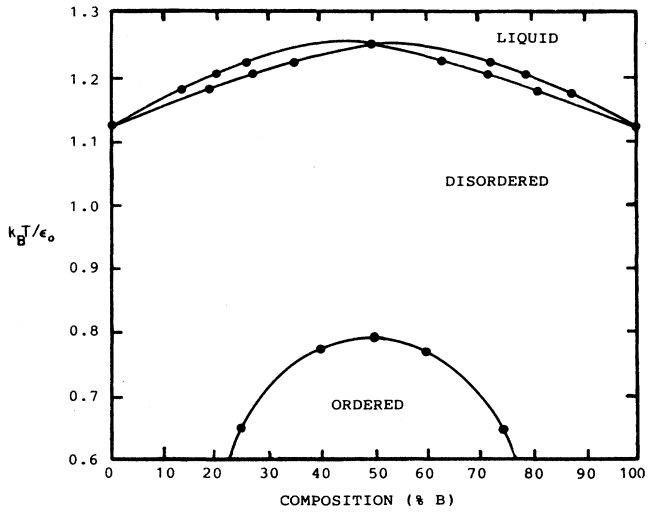

FIG. 2. The complete binary phase diagram corresponding to the symmetric energy assumption (case 1).

tial $\mu_0/\varepsilon_0=-1.5$ for both components. The melting transitions are all of first order, and for the stoichiometric alloy the melting temperature is $k_BT_m/\varepsilon_0=1.23$. The order-disorder transitions are all of second order, and for the stoichiometric alloy the transition temperature is $k_BT_c/\varepsilon_0=0.78$. As expected from the small number of vacancies at these temperatures this transition agrees very well with the reported values from a square-lattice Ising model in a pair approximation.

For the asymmetric phase diagram of Fig. 3 we started from the stoichiometric alloy with values of the chemical potentials:

$$\frac{\mu_A}{\varepsilon_{AA}}=-1.708, \quad \frac{\mu_B}{\varepsilon_{BB}}=-1.114 .$$

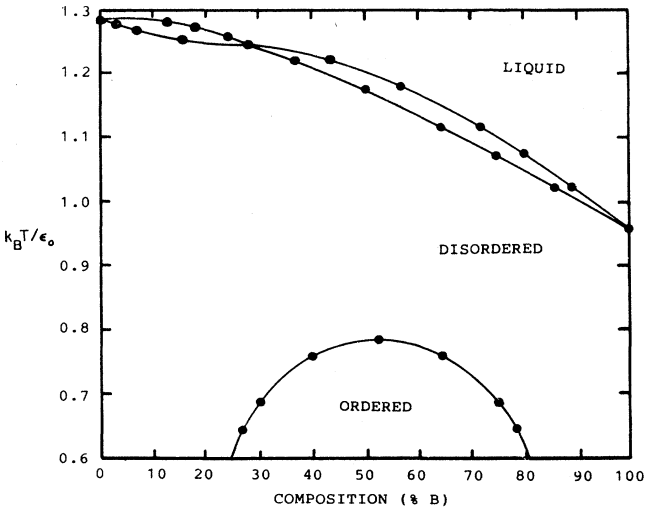

FIG. 3. The complete binary phase diagram corresponding to the asymmetric energy assumption (case 2).

This insured the stoichiometric composition for the solid disordered phase. The parameters of the calculation shown in Table I are such that the ordering energy is the same as in the symmetric phase diagram, and therefore the order-disorder temperature of the stoichiometric composition is the same as in the diagram of Fig. 2. The diagram is, of course, not symmetric about the equiatomic composition in either the solidus, liquidus, or the order-disorder boundaries. It is interesting to note how similar these diagrams are to actual phase diagrams, in spite of the simplicity of the model. This similarity illustrates how the general trends of the present results are expected to have quite general validity in a qualitative way. It is clear, for example, that the present model, when applied to a segregating system instead of an ordering system, will yield a simple eutectic diagram.

B. Grain-boundary ordering transitions

The behavior of the grain-boundary region was studied by computing the density, composition, and long-range order parameter across the grain boundary. For case 1 of a symmetric phase diagram, two types of phenomena were observed as the temperature was increased, namely the disordering of the boundary region and the transformation of the structure to one with increasingly liquidlike properties. This liquidlike structure is shown in Fig. 4 for a stoichiometric alloy of case 1. Note that this behavior is very similar to that obtained for a pure material.[1] The order-disorder transition does not seem to affect this transition significantly. The thickness of the region affected by the presence of the boundary increases logarithmically with temperature and diverges for the melting temperature as discussed by Kikuchi and Cahn[1] for a pure material. The ordering in the alloy is disturbed in the grain-boundary region as shown in Fig. 5, where composition profiles are plotted for a boundary of the stoichiometric alloy in case 1. The oscillations of the composition plane by plane decrease in amplitude in the

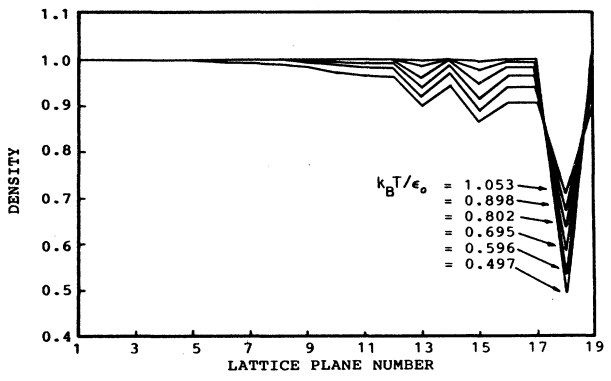

FIG. 4. Density profiles across the grain boundary for several temperatures. The center of the grain boundary is the lattice plane number 19, and the profiles for each temperature are repeated on the right side as a mirror image. The energy assumptions are those of case 1 in the text.

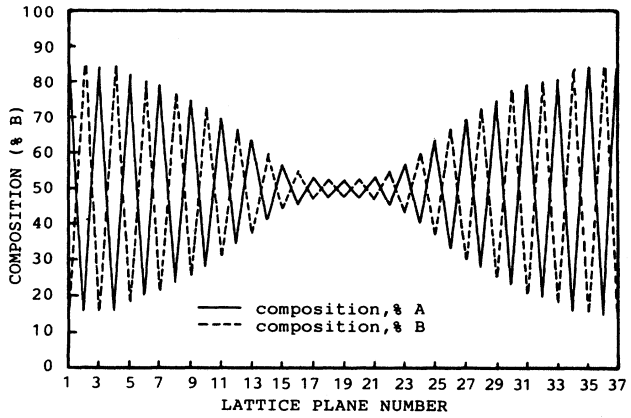

FIG. 5. The composition profile across the grain boundary for the stoichiometric alloy (case 1) at $T/T_c=0.765$.

vicinity of the grain boundary, meaning significantly more disorder. Figure 6 shows the long-range order parameter calculated plane by plane for the stoichiometric alloy in cases 1 and 2. In this figure it can be seen that the stoichiometric alloy disorders more in the case of the symmetric phase diagram than in the asymmetric one. Also the thickness of the disordered layer diverges logarithmically as the order-disorder transition temperature is approached. The present results indicate that although the boundary region is significantly more disordered than the bulk, the actual transition temperature for the boundary is the same as that of the bulk. These results are very similar to those obtained by Foiles for Ni_3Al.[10,11] In particular, the calculated antisite defect energies for Ni_3Al follow the same behavior as the order parameter calculated in the present work in the vicinity of the grain boundary.

In addition to the disordering transition, we observed transitions among the different variants of the grain-boundary structure. These variants correspond to the two possible location types of the grain-boundary plane and are not equivalent in case 2 of the asymmetric diagram. In this case starting with a grain boundary located

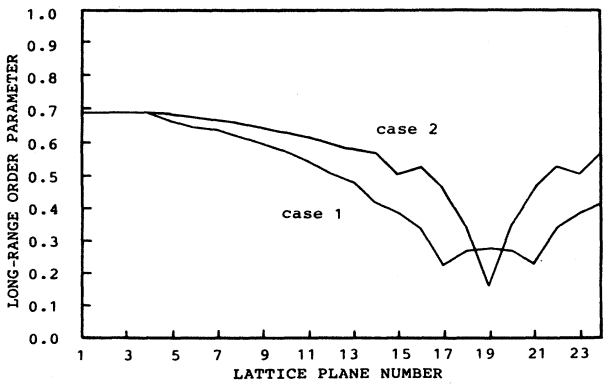

FIG. 6. Long-range order-parameter profiles across the grain boundary for both stoichiometric alloy cases 1 and 2 at $T/T_c=0.765$.

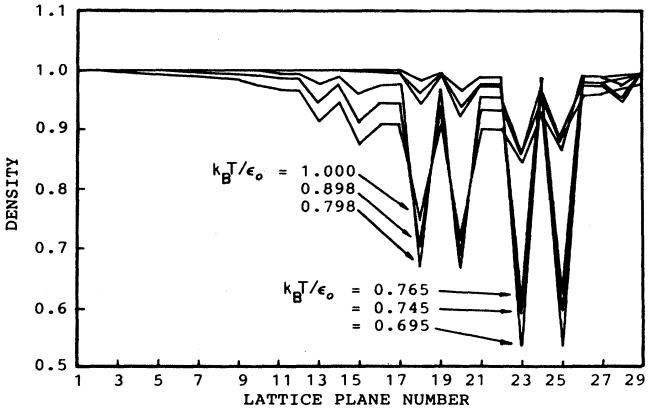

FIG. 7. Density profiles across the grain boundary. In the case of the asymmetric energy assumption (case 2), the center of the grain boundary shifts five planes from the original boundary plane (from 19 to 24) for temperatures above the order-disorder temperature $k_BT/\varepsilon_0=0.875$.

at a plane rich in A atoms at temperatures below the order-disorder temperature, the boundary shifts by five planes to the next coincident plane which is rich in B atoms. This structure has lower energy than the initial location. The same starting configuration subject to the minimization process at temperatures above the order-disorder transition does not present any shift in the boundary plane location. This is shown in the density profiles of Fig. 7. These results indicate that at temperatures higher than the order-disorder transition there is only one variant of the grain boundary, which is a disordered one.

C. Segregation behavior

In Fig. 5 the composition oscillations are such that their average in the bulk is the equiatomic composition. Even though they decrease in amplitude in the grain-boundary region, the average composition is still maintained to be the same as in the bulk. That is, in the

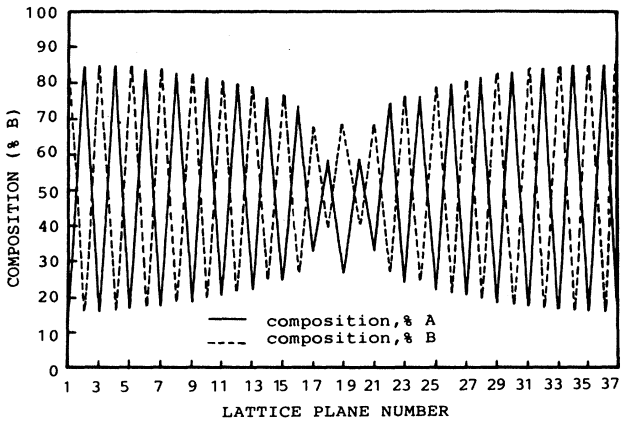

FIG. 8. The composition profile across the grain boundary for the stoichiometric alloy (case 2) at $T/T_c=0.765$.

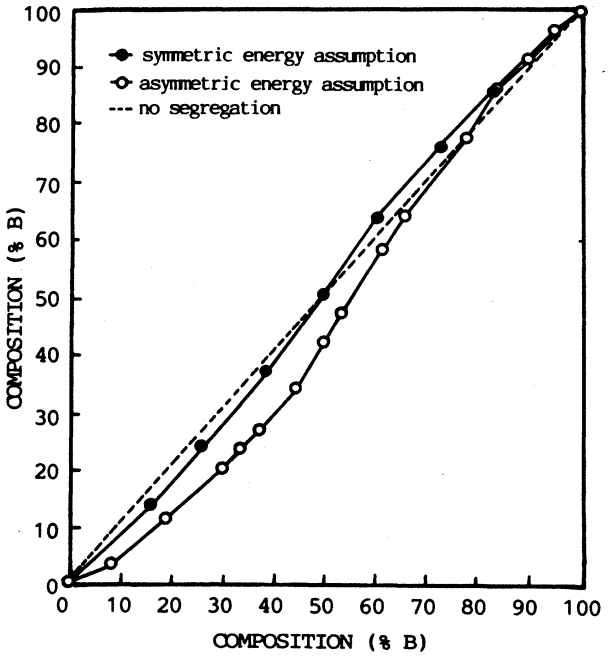

FIG. 9. The plot of the grain-boundary composition as a function of the bulk composition for a $\Sigma=5$ boundary at $T/T_c=0.765$.

stoichiometric alloy for the symmetric phase diagram there is no segregation of either component to the grain boundary. This is not the case for the asymmetric phase diagram or when the composition is varied away from stoichiometry. Figure 8 shows composition profiles for a stoichiometric alloy of type 2 (asymmetric phase diagram case). The oscillations not only decrease but the average is now enriched in the lower-melting-point component. Similar effects can be seen if the composition changes, as shown in Fig. 9. In this figure we plot the composition of the grain boundary as a function of the bulk composition. It is seen that the asymmetry in the phase diagram of the alloys of type 2 is reflected in these results as well. It is important to discuss how the composition of the grain boundary is defined since there are several possible definitions and they may yield different results. We used the composition defined plane by plane, and then the composition of the grain boundary plane itself was averaged with that of the two adjacent planes. Note that when the boundary is located at planes of type *A*, *B* atoms are preferentially removed and vice versa.

IV. DISCUSSION

First we would like to point out that the simple model used can yield complete phase diagrams that are quite similar to actual ones. The model is also adequate to study a variety of grain-boundary phenomena, particularly the high-temperature chemical order and spatial structure.

We would also like to discuss the general implications of the present results for the high-temperature behavior that can be expected in grain boundaries in ordered alloys. It is clear that the results that have been found for surfaces also apply to grain boundaries, that is, there will be a region around the grain boundary more disordered than the bulk. The thickness of this region diverges logarithmically as the order-disorder temperature is approached. Also, segregation effects observed in the vicinity of surfaces will appear in grain boundaries. The disordering phenomenon does not seem to depend strongly on the details of the atomic interaction energies used in the simulation. On the other hand, the type of segregation observed will depend on the phase diagram and therefore the energetic assumptions used in the calculation. The present results show that there will be segregation effects and that they can be very significant. It appears that when high-temperature properties of grain boundaries in ordered alloys are studied, the segregation and disordering effects are essential features that have to be considered.

ACKNOWLEDGMENTS

This work was supported by the Department of Energy, Energy Conversion and Utilization Technologies (ECUT) program under Subcontract No. 19X-89678V with Martin Marietta Energy Systems Inc. and was monitored by Oak Ridge National Laboratories. The authors are thankful to Professor R. Kikuchi for a copy of the code for a one-dimensional case and to Professor Sanchez for many helpful discussions.

[1]R. Kikuchi and J. W. Cahn, Phys. Rev. B **21**, 1893 (1980).
[2]P. Deymier and G. Kalonji, J. Phys. C **4**, 213 (1985).
[3]R. Kukuchi (unpublished).
[4]J. L. Moran-Lopez and J. M. Sanchez, Phys. Rev. Lett. **57**, 360 (1986).
[5]J. M. Sanchez, J. R. Barefoot, R. N. Jarrett, and J. K. Tien, Acta Metall. **32**, 1519 (1984).
[6]T. Takasugi and O. Izumi, Acta Metall. **31**, 187 (1983).
[7]R. Kikuchi and J. W. Cahn, Phys. Rev. B **36**, 418 (1987).
[8]R. Kikuchi, J. Phys. (Paris) **38**, C7-307 (1977).
[9]L. Moran-Lopez, F. Mejia-Lira, and K. H. Bennemann, Phys. Rev. Lett. **54**, 1936 (1985).
[10]S. M. Foiles, Mat. Res. Soc. Symp. Proc. **81**, 51 (1987).
[11]S. M. Foiles and M. S. Daw, J. Mater. Res. **2**, 5 (1987).